CrossMark

ORIGINAL PAPER

Polypropylene/short glass fiber/nanosilica hybrid composites: evaluation of morphology, mechanical, thermal, and transport properties

Nanoth Rasana[1] · Karingamanna Jayanarayanan[1,2]

Abstract In this work, the effect of incorporation of glass fiber and nanosilica separately and in combination in a thermoplastic matrix is investigated. Individual micro, nano, and hybrid multiphase composites based on polypropylene were prepared via twin screw extrusion followed by injection molding. The glass fiber content was maintained at 10 wt% and nanosilica level was fixed at 4 wt%. The microstructure of the hybrid composite indicated the presence of nanosilica surrounding the glass fibers. Higher tensile strength and modulus was reported for hybrid composite, followed by micro and nanocomposite. The differential scanning calorimetry studies suggested that the presence of glass fibers could hasten the crystallization of PP in comparison with nanosilica. The thermal degradation studies for hybrid composite exhibited a prominent thermal stability. The delayed diffusion of solvent in hybrid composite was observed due to the confinement regions generated by the combination of micro and nanofillers.

Keywords Hybrid composite · Glass fibers · Nanosilica · Transcrystallization · Permeability

✉ Karingamanna Jayanarayanan
kj_narayanan@cb.amrita.edu; kjnarayanan@gmail.com

1 Department of Chemical Engineering and Materials Science, Amrita School of Engineering, Amrita Vishwa Vidyapeetham, Amrita University, Coimbatore, Tamil Nadu 641112, India

2 Center of Excellence in Advanced Materials and Green Technologies (CoE-AMGT), Amrita Vishwa Vidyapeetham, Amrita University, Coimbatore, Tamil Nadu 641112, India

🅢 Springer

Introduction

Reinforced polymers have wide applications in the field of automotive, aerospace, consumer electronics industry, etc. Nowadays, a lot of studies are being carried out using new type of reinforcements in polymer matrices [1, 2]. Polypropylene which is cheaper in comparison with many other thermoplastic counterparts has always been an option for composites industry owing to the versatility in the techniques used for processing and recyclability [3]. Over the years, wide variety of fillers in the form of nano and micropowder, particles, flakes, fibers, platelets, etc. short and long glass fibers [4, 5] nanosilica [6, 7], nanoclay [8, 9], carbon nano fibers, single [10] and multi walled carbon nanotubes [11], graphite nanoplatelets [12], and natural fibers such as wood fibers [13–15], flax [16, 17], and sisal fibers [18] are incorporated in matrices.

Studies on glass fiber reinforced polypropylene composites were carried out and their mechanical performance was evaluated by Barré et al. [19]. The incorporation of nanoclay in glass fiber reinforced PP composites was reported by Rahman et al. [9]. Karmarkar et al. reported the incorporation of wood fiber in PP [20]. Palza et al. introduced spherical and layered silica nanoparticles in PP and at very low concentrations of filler loading, a better mechanical reinforcement was reported [7]. At higher concentrations of fillers, an adverse effect on composite properties due to the formation of nanoagglomerates was also detailed. The properties of carbon fiber reinforced PP composites were analyzed and characterized by Shazed et al. [10].

The collective contribution of nano and microfillers in reinforcement of a polymer matrix is expounded as the hybrid effect [21, 22]. Rahman et al. [9] reported the hybrid effect of glass fiber and nanoclay in PP on the flexural and tensile properties of the composites. The hybrid reinforcement effect and surface treatment of carbon nanotubes with silane in short glass fiber reinforced PP composites was revealed by Karsili et al. [3]. A better electrical conductivity of the composites was also reported with increased nanotube loading [3]. The transport behavior of water in PP-based natural cellulosic fiber composites was discussed in the literature [23]. The water absorption coefficients of recycled newspaper/glass fiber reinforced PP hybrid composites were reported by Shakeri et al. [24].

It was observed that water absorption decreased with the incorporation of kaolin filler in PP/Rattan powder/Kaolin hybrid composites [25]. It was also revealed that moisture absorption decreased with the increase of glass fiber content than the incorporation of hydrophilic natural short hemp fiber in PP/hemp fiber/glass fiber hybrid composite [26]. Studies on solvent sorption of PP composites with multiscale fillers are not reported yet.

The recent studies are now focused on the synergistic contribution of micro and nanofillers by introducing them in a single matrix and thereby achieving property enhancement [27, 28]. The better distribution of the fillers is the crucial solution for optimal transfer of load when a composite is subjected to external forces. The agglomeration of fillers reduces the mechanical properties as they act as stress riser regions [27–29]. For better dispersion of fillers, surface treatment using silanes and

incorporation of maleic anhydride compatibilizers are commonly employed [30–32].

This work is primarily focused on the comparison of morphology, mechanical, thermal, and sorption behavior of polypropylene (PP), polypropylene/glass fiber (PPG), polypropylene/nanosilica (PPN), and polypropylene/glass fiber/nanosilica (PPGN) composites. Although the mechanical and morphological properties of hybrid composites are reported crystallization and sorption, characteristics of multiphase hybrid composites are not discussed widely. The dispersion of glass fiber and nanoparticles which has vital importance in the development of hybrid composites can be studied by morphology analysis using SEM and TEM. An effort has been made to explicate the stress–strain relationship and other tensile properties. An attempt has been laid down to study the thermal properties using DSC and thermal stability of the composites using thermogravimetric analysis. The transport behavior of the composites is also being examined to study the variation in diffusivity with hybrid filler reinforcement. Microfillers when added in polymers require higher loading levels to achieve better performance. The inclusion of nanoscale filler along with micro fillers offers potential for enhanced mechanical, thermal, and barrier properties with regard to conventionally filled composites. Elevated mechanical properties, and improved thermal and barrier properties are expected from hybrid composites in comparison with micro and nanocomposites.

Materials and experimental

The materials used for composite preparation were polypropylene in the form of beads (Repol of grade H110MA, Reliance India, melt flow index: 11.0 g/10 min: melting temperature: 167.7 °C), powdered SiO_2 nanosilica particles (Nanowings India, average primary particle size: <100 nm, purity: 99%), and flat glass fiber (Brakes India Ltd., India) of length 3 mm and width 1 mm. A master batch of nanosilica in PP was prepared using an internal mixer before extrusion. The lumps of masterbatch thus obtained were consolidated into the form of thin sheets using a hydraulic compression press. These sheets were then sliced into thin pellets and preheated polypropylene samples were then mixed with varying proportions of nanosilica and glass fiber and the mixture is melt compounded in a counter rotating twin screw extruder (screw diameter: 25 mm and *L/D* ratio: 30:1) equipped with a die to bring forth a strand of diameter 2 mm. The temperatures maintained across the feed to die zones of the screw were 150, 170, 190, 200, and 210 °C, respectively, and a screw speed of 100 rpm was set for all runs. The composites were designated as PP, PPG, PPN, and PPGN with respect to their compositions and are mentioned in Table 1.

Table 1 Sample nomenclature for individual and hybrid composites

Sample type	Polypropylene (PP) (wt%)	Glass fiber (G) (wt%)	Nanosilica (N) (wt%)	Sample code
Neat polymer	100	0	0	PP
Micro composite	90	10	0	PPG
Nano composite	96	0	4	PPN
Hybrid composite	86	10	4	PPGN

The pelletized composites are then injection molded in a Ferromatik Milacron-Sigma 50T injection molding machine to form dumb bell-shaped test specimens.

Characterization methods

The surface morphology of the composites was analyzed using JEOL JSM-6490 LASEM. For SEM analysis the sample surface, PPGN was first treated with hot xylene and then well polished. Before scanning, specimen was cleaned with blown air and sputtered with gold–palladium of thickness less than 3 nm for 90 s. Morphological structure and dispersion of nanosilica in PP was characterized by Jeol/JEM 2100 TEM with an acceleration voltage of 200 kV. Ultrathin slices of injection molded nanocomposites were prepared and placed on heated copper grid for analysis. The tensile tests were performed at a constant cross head speed of 50 mm/min using Zwick tensile testing machine. The thermal parameters of neat PP and other composites were studied using a DSC Q20 V24.10 Build 122 make differential scanning calorimeter and the thermal decomposition tests of the composites were done using SDT Q600 V20.9 Build 20 TGA analyzer. The heating and cooling rate were maintained as 10 °C/min.

For sorption studies, square samples of size 20×20 mm^2 were cut and the edges are curved to achieve uniform sorption of solvent. The samples were fully immersed in xylene, and at successive time intervals, samples were picked out of the solvent and rub out the excess solvent with a filter paper. The samples were then weighed and this procedure was continued until the equilibrium solvent sorption was achieved. The mol% uptake Q_t of solvent was calculated by an expression:

$$Q_t\,(\%) = \frac{\left(\frac{\text{Sorbed solvent mass}}{\text{solvent molar mass}}\right)}{\text{Initial mass of sample}} \times 100. \tag{1}$$

Fig. 1 TEM images of nanocomposite at **a** 50 nm, **b** 20 nm (magnified), and **c** 50 nm resolution
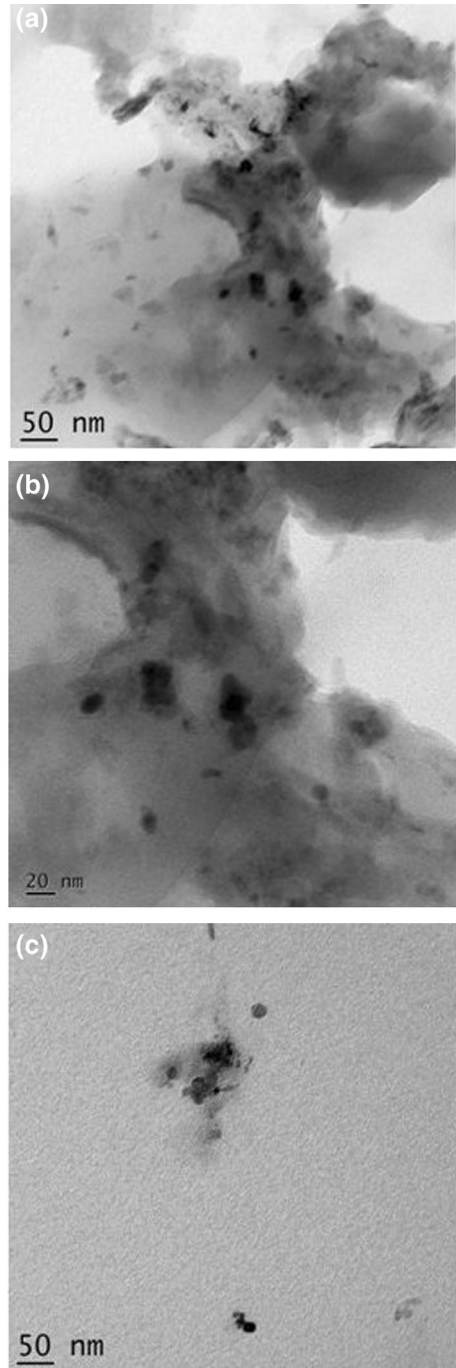
Results and discussion

Morphology development

Transmission and scanning electron microscopy

TEM images of PPN composite in Fig. 1a–c gave insights to the distribution of nanoparticles in PP base matrix. The dark region in the figures represents nanosilica particles and is observed that at some regions, nanosilica was properly dispersed, and at certain locations, nanosilica aggregates were seen. Aggregates of nanosilica would have formed due to its strong tendency to agglomerate by van der Waals force of attraction. It has been reported that the high shear rate in twin screw extruder can reduce the agglomeration tendency of the particles to a large extent. The shear forces maintained during the extrusion process force the polymer chains to separate the nanoparticles and distribute them in the matrix [29, 33].

The SEM images of hybrid composite at a magnification of 500× and 1000×, as shown in Fig. 2a, b, indicate that flat short glass fibers are properly dispersed in PP matrix, and this would have raised the ability of the composite to transfer load to the matrix upon the application of external force. Owing to the high shear of mixing during extrusion, the *L/D* ratio of glass fibers would have reduced which could act as a drawback in the improvement of mechanical properties.

A magnification of 1500× and 2500×, as shown in Fig. 2c, d, distinctly shows the morphology of glass fiber embedded in the base matrix. When an individual glass fiber embedded in PP is viewed at a higher magnification, Fig. 2e, it is seen that nanoparticles are attached on the edges and on the surface of the glass fiber that are observed as white spherical particles. Thus, it is inferred that the effective dispersion of nanosilica took place. In Fig. 2e, a good spread of nanoparticles on the surface of glass fiber can be observed. A slight agglomeration of nanoparticles can also be viewed in Fig. 2e because the inherent nature of nanoparticles is to bundle themselves due to high van der Waals force of attraction [6, 33].

Mechanical properties

As shown in Table 2, the tensile studies indicate an ultimate tensile strength of 35 MPa for neat PP and exhibited an elongation at break of 20%. With the inclusion of inorganic glass fiber, tensile strength of the PP was increased by 7 MPa and the modulus has increased from 1200 to 2300 MPa which improved the stiffness of the composite. The better distribution of glass fibers in the PP matrix and the strong adhesion between PP and glass fiber would have contributed to the improved stiffness and strength [16, 34].

As shown in stress–strain graph, Fig. 3, it is evident that the inclusion of glass fibers greatly reduced the tendency of PP to undergo plastic deformation which is confirmed with the reduced elongation at break of 8.5% (lessened by 16.5%) and makes the composite brittle. However, with the inclusion of nanosilica in PP, the elongation at break is reduced only to 15% which exhibits a more ductile type of
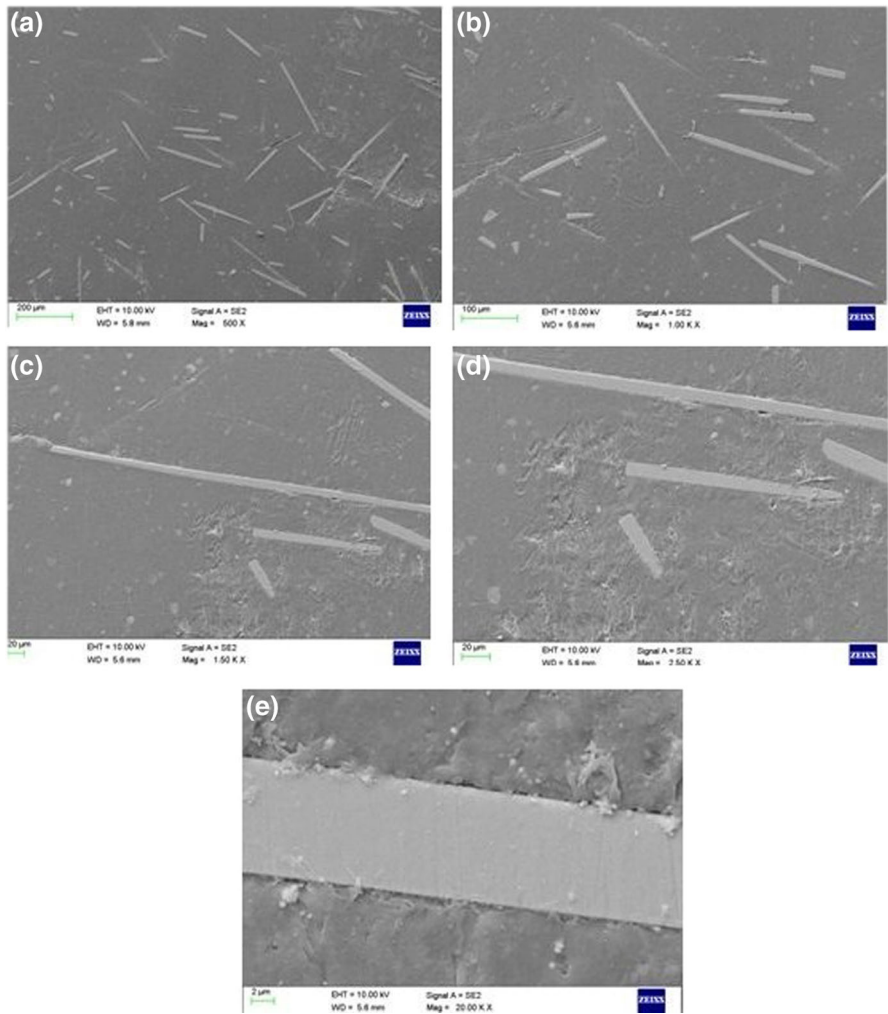
Fig. 2 SEM micrographs of hybrid composite (**a**, **b**, **c**, **d**). Glass fibers dispersed in PP matrix at different magnifications; (**e**) an individual glass fiber embedded in PP matrix surrounded by nanosilica

Table 2 Tensile properties of PP, micro, nano, and hybrid composites

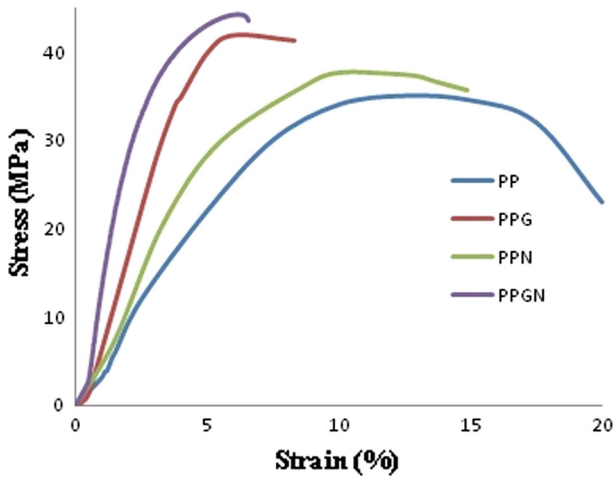| Composite	Ultimate tensile strength (MPa)	Young's modulus (GPa)	Elongation at break (%)
PP	35 ± 0.9	1.2 ± 0.1	20 ± 1.9
PPG	42 ± 1.2	2.3 ± 0.4	8.5 ± 0.6
PPN	36.8 ± 1.1	1.3 ± 0.2	15 ± 1.3
PPGN	44 ± 1.4	2.6 ± 0.5	7.7 ± 0.8

Fig. 3 Stress–strain curves of PP, micro, nano, and hybrid composite

failure. With the incorporation of 4 wt% nanosilica in PPG composite, plastic deformation to failure further reduced to 7.7% which establishes the brittleness of the hybrid composite. This could be due to the obstructions offered by the micro and nanofillers to the mobility of polymer chains on the application of a tensile force. The percentage increase in tensile strength and modulus of the hybrid composite are 25.7 and 116.6%, respectively, with respect to PP.

Differential scanning calorimetry

The melting and crystallization characteristics of composites such as melting (T_m), peak crystallization (T_p) temperatures, onset and end set temperatures of crystallization (T_o and T_e), maximal crystallization time (time to crystallize from onset to peak crystallization temperature, t_{max}), under cooling temperature (melting and peak crystallization temperature difference, ΔT_C), and time for half crystallization ($t_{1/2}$) obtained are reported in Table 3.

The onset and endset temperature of crystallization is the highest for the hybrid composite (PPGN) when compared to the individual composites PPG, PPN, and

Table 3 Thermal properties of PP phase in neat PP, PPG, PPN, and PPGN composites obtained from DSC analysis

Sample	T_m (°C)	T_o (°C)	T_e (°C)	T_p (°C)	$t_{1/2}$ (s)	ΔT_C (°C)	t_{max} (s)	X_c (%)
PP	167.99	118.19	99.58	110.19	56	57.8	55.2	58.2
PPG	169.62	122.63	109.6	117.36	38.6	46.99	36.20	66.8
PPN	166.12	120.97	107.32	114.07	40.9	52.05	44.79	63.2
PPGN	167.69	124.63	111.88	118.83	38.79	48.85	39.19	68.9

virgin PP. With the addition of 10 wt% of glass fiber to virgin PP, it is observed that the onset of crystallization occurred 4 °C ahead than pure PP. However, with the inclusion of nanosilica in virgin PP, the onset of crystallization occurred at 120.97 °C which means that the beginning of crystallization gets delayed by 1.66 °C when compared with PPG. This shows that the addition of long glass fibers has initiated the nucleating effect and each glass fiber acts as a nucleating site in PP. The heterogeneous inclusion of nanosilica in PP and glass fiber enhances crystallization with the formation of spherulites, and nanosilica acts as an excellent nucleating agent in PP [35, 36]. The synergistic effect of glass fiber and nanosilica in the hybrid composite speeds up the crystallization of PP and the crystallization commences 6 °C earlier, than virgin PP.
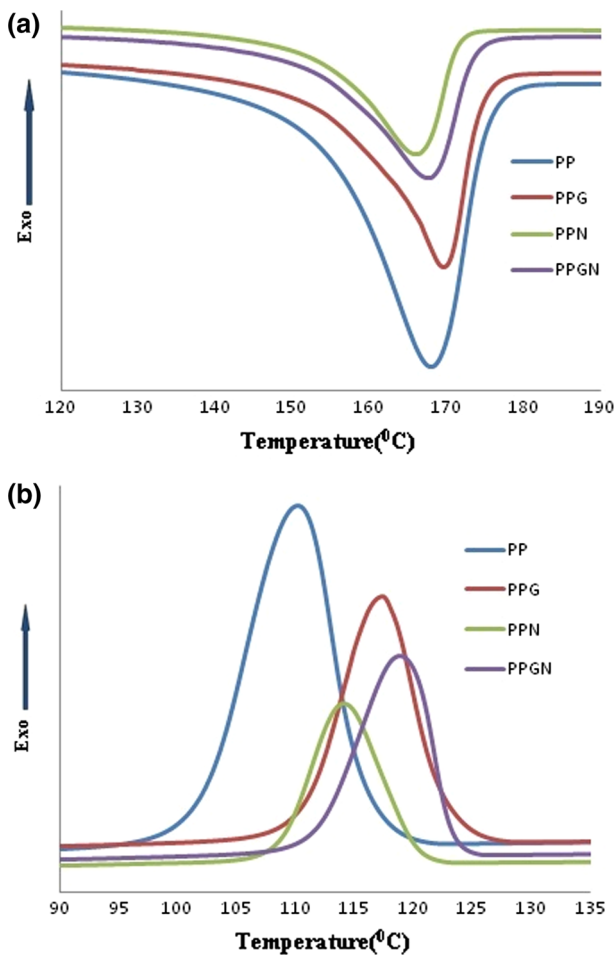

Fig. 4 a DSC heating thermograms of PP, PPG, PPN, and PPGN composites **b** DSC cooling thermograms of PP, PPG, PPN, and PPGN composites

As shown in Fig. 4a, b for the hybrid composite, there is a significant advancement in the peak crystallization temperature and the same occurred 8.64 °C ahead of neat PP [37]. The heterogeneous inclusion of nanosilica in PPG composite reduces the melting temperature of hybrid composite which indicates the formation of imperfect PP crystals with the inclusion of fillers [38].

It is well known that transcrystallization is an important phenomenon seen in fiber reinforced crystallizable plastics like PP [37–39]. Shish–kebab structure has been described in the case of PP reinforced with glass [40], carbon nanotube
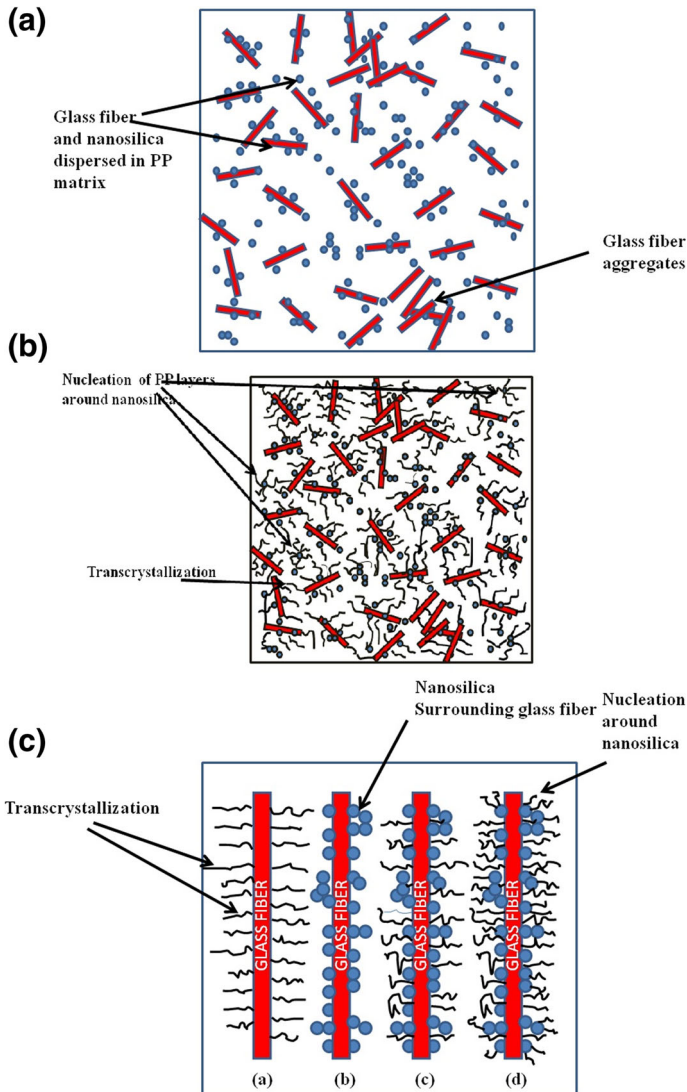

Fig. 5 Illustration indicating dispersion of **a** hybrid fillers in PP matrix and **b** heterogeneous nucleating effect of nanosilica **c** transcrystallization effect of glass fiber

[39, 40], etc. A schematic of micro and nanofillers dispersed in PP is shown in Fig. 5a. As evident from the scheme, nanosilica preferably locates around glass fibers encourages heterogeneous nucleation of PP around it. On the other hand, it might impede the growth of transcrystalline layer of PP, which is illustrated in Fig. 5b. The presence of glass fiber in PP leads to the transcrystallization effect as represented in Fig. 5c. The half crystallization time for PPG and PPGN composites is lower than virgin PP and PPN which is manifested as a narrow peak of crystallization and higher degree of crystallinity. In addition, the melting and the peak crystallization temperature difference is less for PPG and PPGN which indicate the effectiveness of glass fiber in accelerating the crystallization process and can be inferred that nanosilica alone cannot contribute immensely in hastening the crystallization process.

An equation used to calculate the crystallinity of the PP is presented below [41]:

$$X_C = \left[\frac{\Delta H_f \times 100}{\Delta H_f^0 \times x} \right]. \tag{2}$$

The value of ΔH_f^0 (the latent heat of fusion of 100% crystalline PP) was used as 207 J/g and 'x' is the weight fraction of polypropylene in the composite. A relation to calculate the percentage relative crystallinity [41] (X_T) is as shown below:

$$X_T = \left[\frac{\int_{T_0}^{T} \left(\frac{dH}{dt}\right) dt}{\int_{T_0}^{T_e} \left(\frac{dH}{dt}\right) dt} \right] \times 100, \tag{3}$$

where (dH/dT) is the liberation rate of heat.

From Fig. 6a, b, it is observed that at a specified temperature, the relative crystallinity is highest for the hybrid composite and the completion of crystallization of PP in hybrid composite happened few seconds before the PPG composite. Due to the growth of PP spherulites around nanosilica, the contribution of nanosilica in crystallization of PP is pronounced towards the latter half of the process.

Thermal decomposition

Thermal degradation characteristics of the composites are compared with neat PP and are reported in Table 4. T_{onset}, $T_{10\%}$, and $T_{50\%}$ represent the onset of decomposition, and decomposition temperature at a weight loss of 10 and 50%, respectively. T_{max} indicates the peak temperature at the maximum weight loss rate (dW/dt)$_{max}$. The yield of char at 600 °C was also determined. The TGA thermograms were plotted as shown in Fig. 7a, b

The onset of thermal degradation of neat PP was obtained at 409.4 °C. By introducing inorganic glass fibers into neat PP matrix, the degradation onset shifted by 6.23 °C which reveals the impediments offered by them in thermal break down of the composite. The well-dispersed glass fibers could be mechanically interlocked
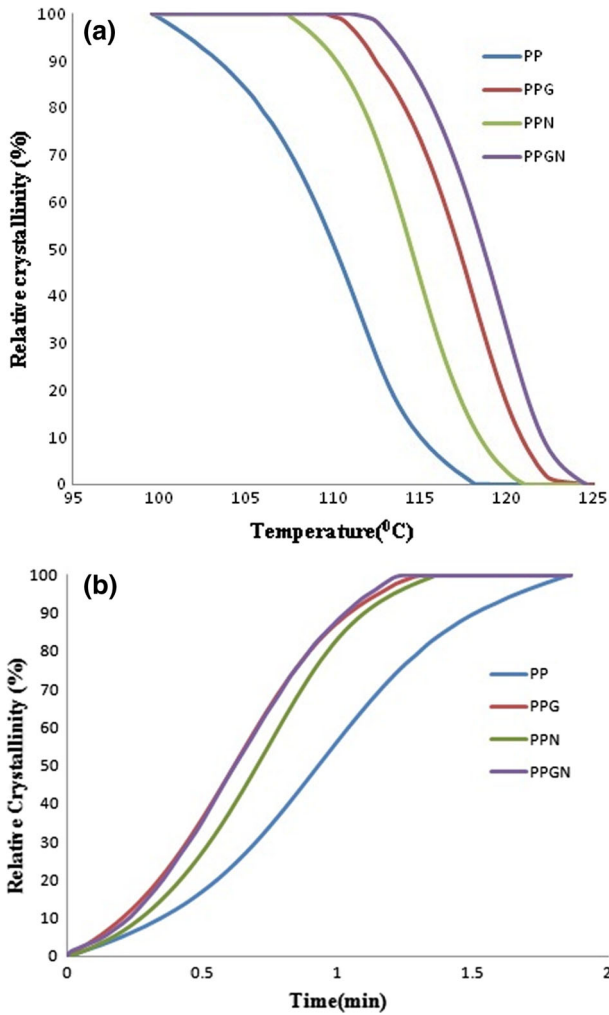
Fig. 6 a Variation of relative crystallinity of pure PP and PP phase in micro, nano, and hybrid composites with temperature. **b** Variation of relative crystallinity of pure PP and PP phase in micro, nano, and hybrid composites with time

Table 4 Non-isothermal degradation characteristics of PP, PPG, PPN, and PPGN composites

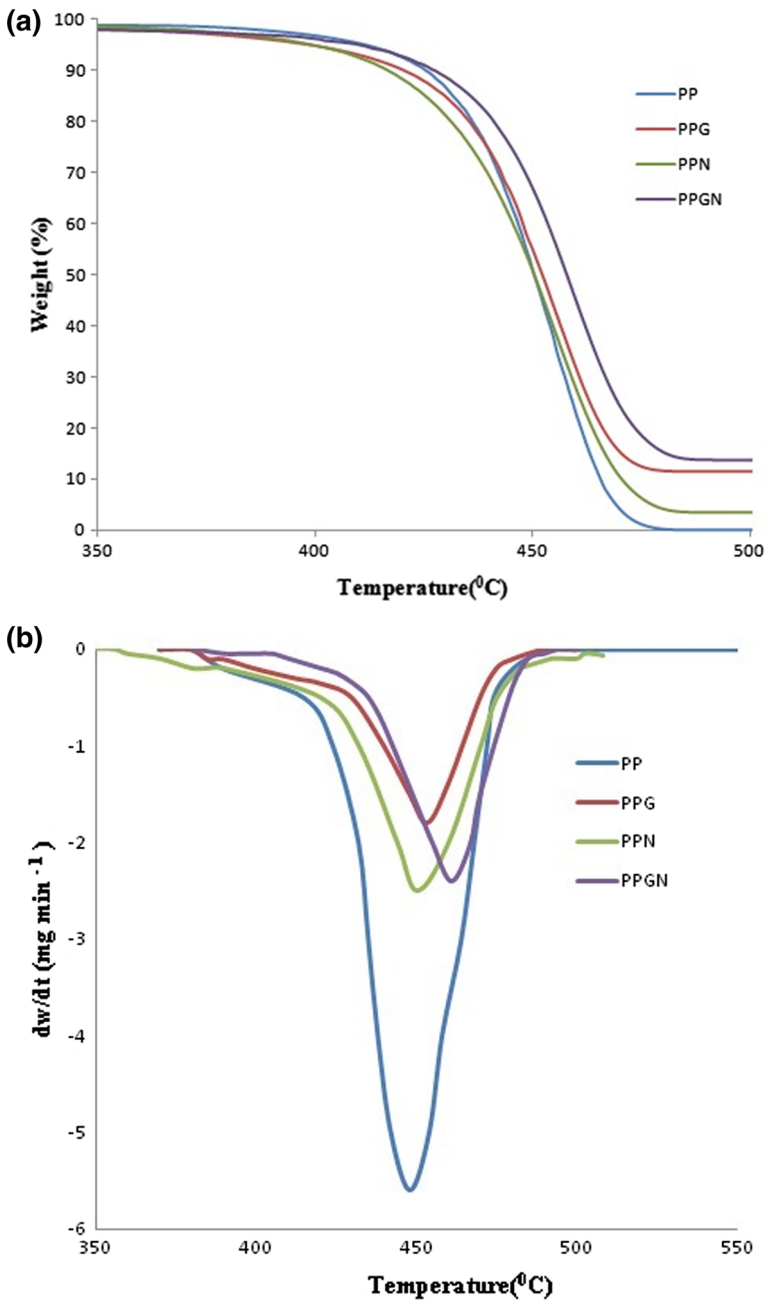| Sample	T_{onset} (°C)	$T_{10\%}$ (°C)	$T_{50\%}$ (°C)	DT_{max} (°C)	$(dW/dt)_{max}$ (%/min)	Char yield at 600 °C (wt%)
PP	409.4	428	452	448.8	22.8	0
PPG	415.6	424	454	453.5	23.3	14
PPN	413.3	418	452	450.2	24.1	4.3
PPGN	427.2	432	460	461.4	23.8	18.8

Fig. 7 a Dynamic TG profiles of PP, PPG, PPN, and PPGN composites. **b** Derivative thermograms for PP, PPG, PPN, and PPGN composites

with PP fibers improving both thermal and mechanical properties [38]. The glass fibers could very well act as a thermal barrier which delays the decomposition of the matrix layer surrounding them [9]. As delineated in Fig. 7b, the significant shift in the onset of thermal decomposition (427.3 °C) for the hybrid composite is an indication of higher thermal stability of PPGN composite.

The addition of nanosilica has also shifted the shoulder of the degradation thermogram to the right, but the effect is pronounced in its synergistic contribution with microfiller. The same decomposition trend is observed at a weight loss of 10 and 50%, respectively. It is noted that at a weight loss of 10%, the individual effect of fillers is not substantial. The PPG and PPN have thermal stability up to 424 and 418 °C, respectively. However, the synergistic effect of glass fiber and nanosilica enhanced the thermal stability to 432 °C. At a weight loss of 50%, the individual effect of nanosilica coincides with neat PP and both records a decomposition temperature of 452 °C, and the hybrid effect of fillers reveals the highest decomposition temperature of 460 °C. For the hybrid composite, the maximum weight loss rate of 23.82%/min was obtained at 461.41 °C, the maximum amongst all samples as seen in Fig. 7b.

A possible reason for the reduction in expected thermal stability of PPN composites could be the regions of agglomeration of nanoparticles as revealed by TEM images. At 600 °C, no char residues were left out for PP, whereas the other three composites left out an appropriate yield of char after decomposition as reported in Table 4.

Sorption studies

The sorption tests were carried out at room temperature. The sorption coefficient can be expressed as follows:

$$S = \frac{W_\infty}{W_P}, \tag{4}$$

where W_α is the solvent mass absorbed at equilibrium swelling and W_P is the initial weight of the composite [42]. From a graph of mol% uptake (Q_t) of solvent versus $t^{1/2}$, for each sample, a master curve is formed which is linear initially. The equation used to calculate diffusivity (D) is given as follows:

$$D = \Pi \left(\frac{t\theta}{4Q_\alpha} \right)^2, \tag{5}$$

where 't' is the fixed thickness of sample (3 mm) and 'θ' is the slope of the linear portion of the master curves. 'Q_α' denotes the equilibrium xylene uptake by the sample. The permeability can be evaluated from diffusivity and sorption coefficient as follows [42]:

$$P = D \times S, \tag{6}$$

where 'S' is the solubility.

Table 5 Diffusivity, sorption coefficient, and permeability of neat PP, individual, and hybrid composites at room temperature

Sample	Diffusivity $\times 10^{-9}$ (D) (m^2/s)	Sorption coefficient (S)	Permeability $\times 10^{-11}$ (P) (m^2/s)
PP	1.9	0.031	5.8
PPG	1.2	0.028	3.7
PPN	1.3	0.039	4.6
PPGN	0.8	0.035	2.9

Table 5 indicates the lowest value of permeability and diffusivity of 2.9×10^{-11} and 0.8×10^{-9} m^2/s, respectively, for hybrid composite due to the higher resistance offered by micro and nanofillers for the penetration of solvent. The microcomposite with the high aspect ratio and the flat nature of the glass fibers offers more impediments to the transport of solvents. The randomness in the distribution of the microlevel fibers can hinder the solvent penetration easily. Whereas in PPN composite, there could be regions where they are not uniformly distributed and tend to aggregate and could be a reason leading to the higher diffusivity of the solvent with respect to PPG.

From Fig. 8, it can be inferred that the solvent uptake is the least for hybrid composite. Due to the presence of multiphase fillers (micro and nano level), the solvent has to follow a tortuous path within the sample and this limits the amount of solvent that can be sorbed.

A scheme for the diffusion of solvent through composites is represented in Fig. 9a–c. The random distribution of glass fibers coupled with the presence of nanosilica develops confinement regions. It is extremely difficult for the solvent to penetrate through these "confinement region", as illustrated in Fig. 9c
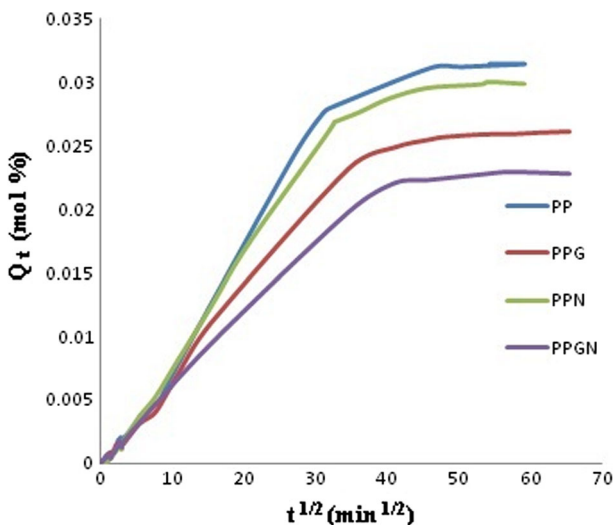
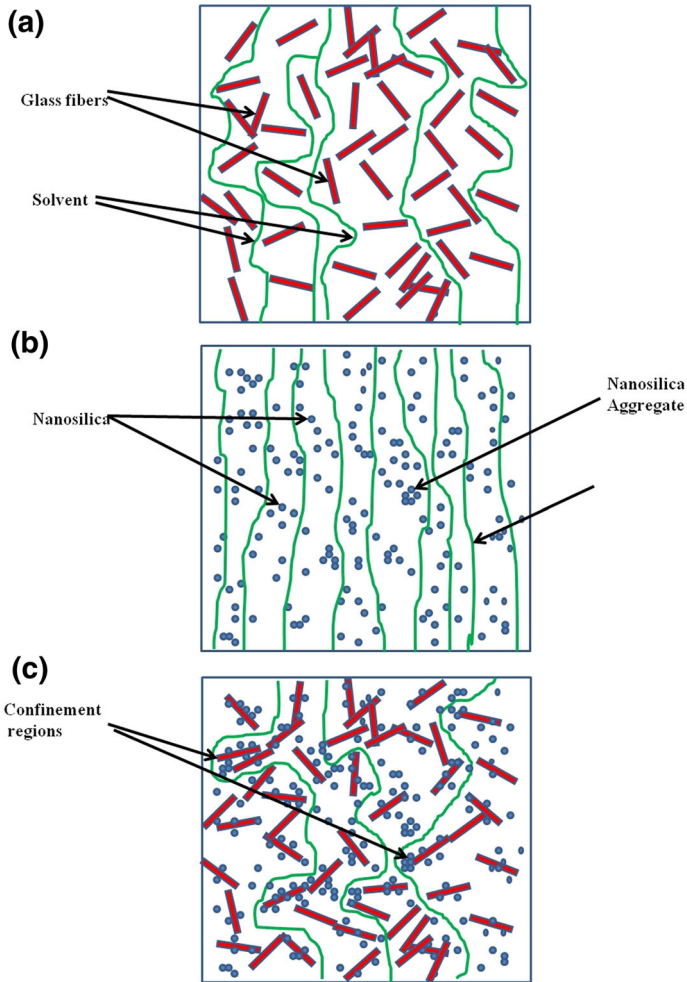**Fig. 8** Sorption curves for neat PP, individual, and hybrid composites at room temperature

Fig. 9 Scheme indicating the diffusion of solvent through **a** micro **b** nano and **c** hybrid composite

Conclusion

- From the microstructure analysis of the hybrid composite, it is inferred that the

  high shear stresses prevalent during mixing could disperse the nanoparticles and large number of them are found to be surrounding the glass fibers.
- The tensile strength of the hybrid composite increased by 26% when compared to base matrix, whereas the increase in tensile modulus is found to be 116%.
- To enhance relative crystallinity of PP phase, the transcrystallization effect of glass fiber was superior to the heterogeneous nucleating effect of nanosilica. PPG composite attains 100% relative crystallinity at a temperature of 111.5 °C in regard with PPN composite which is attained at 107.5 °C. The hybrid effect of

the fillers has contributed to attain 100% relative crystallinity in 72 s in comparison with 111 s of neat PP.

- The synergism of glass fiber and nanosilica is noticeable in thermal degradation studies. The individual incorporation of glass fiber and nanosilica has not enhanced the thermal stability till 50% weight loss of the composite. On the other hand, hybrid composite evinced resistance to thermal degradation as they manifested a temperature of 460 °C for 50% degradation vis-a-vis 452 °C for PP.
- The confinement regions caused due to the dispersal of micro and nanosize fillers could remarkably decrease the transport of the solvent through the polymer. The permeability of hybrid composite has reduced from 5.8×10^{-11} to 2.9×10^{-11} m^2/s due to these confinement regions.

References

1. Zhang J, Chaisombat K, He S, Wang CH (2012) Glass/carbon fibre hybrid composite laminates for structural applications in automotive vehicles. In: Subic A, Wellnitz J, Leary M, Koopmans L (eds), Sustainable automotive technologies. Proceedings of the 4th International Conference. Berlin, Heidelberg: Springer Berlin Heidelberg, pp 69–74
2. Heinemann MD, von Maydell K, Zutz F, Kolny-Olesiak J, Borchert H, Riedel I et al (2009) Photo-induced charge transfer and relaxation of persistent charge carriers in polymer/nanocrystal composites for applications in hybrid solar cells. Adv Funct Mater 19(23):3788–3795
3. Gamze Karsli N, Yesil S, Aytac A (2014) Effect of hybrid carbon nanotube/short glass fiber reinforcement on the properties of polypropylene composites. Compos B Eng 63:154–160
4. Thomason JL, Vlug MA (1996) Influence of fibre length and concentration on the properties of glass fibre-reinforced polypropylene: 1. Tensile and flexural modulus. Compos A Appl Sci Manuf 27(6):477–484
5. Unterweger C, Brüggemann O, Fürst C (2014) Effects of different fibers on the properties of short-fiber-reinforced polypropylene composites. Compos Sci Technol 103:49–55
6. Jacob S, Suma KK, Mendaz JM, George A, George KE (2009) Modification of polypropylene/glass fiber composites with nanosilica. Macromol Symp 277(1):138–143
7. Palza H, Vergara R, Zapata P (2011) Composites of polypropylene melt blended with synthesized silica nanoparticles. Compos Sci Technol 71(4):535–540
8. Mohan T, Kanny K (2010) Influence of nanoclay on rheological and mechanical properties of short glass fibre reinforced polypropylene composites. J Reinf Plast Compos 30(2):152–160
9. Rahman NA, Hassan A, Yahya R, Lafia-Araga R, Hornsby P (2012) Polypropylene/glass fiber/nanoclay hybrid composites: morphological, thermal, dynamic mechanical and impact behaviors. J Reinf Plast Compos 31(18):1247–1257
10. Shazed MA, Suraya AR, Rahmanian S, Salleh MA (2014) Effect of fibre coating and geometry on the tensile properties of hybrid carbon nanotube coated carbon fibre reinforced composite. Mater Des 54:660–669
11. Taraghi I, Fereidoon A, Zamani MM, Mohyeddin A (2015) Mechanical, thermal, and viscoelastic properties of polypropylene/glass hybrid composites reinforced with multiwalled carbon nanotubes. J Compos Mater 49(28):3557–3566
12. Bhattacharya M (2016) Polymer nanocomposites—a comparison between carbon nanotubes, graphene, and clay as nanofillers. Materials 9(4):262
13. Bledzki AK, Gassan J (1999) Composites reinforced with cellulose based fibres. Prog Polym Sci 24(2):221–274

14. Wambua P, Ivens J, Verpoest I (2003) Natural fibres: can they replace glass in fibre reinforced plastics? Compos Sci Technol 63(9):1259–1264

15. Tomlal EJ, Thomas PC, George KC, Jayanarayanan K, Joseph K (2010) Impact, tear, and dielectric properties of cotton/polypropylene commingled composites. J Reinf Plast Compos 29(12):1861–1874

16. Arbelaiz A, Fernández B, Cantero G, Llano-Ponte R, Valea A, Mondragon I (2005) Mechanical properties of flax fibre/polypropylene composites. Influence of fibre/matrix modification and glass fibre hybridization. Compos A Appl Sci Manuf 36(12):1637–1644

17. Cantero G, Arbelaiz A, Llano-Ponte R, Mondragon I (2003) Effects of fibre treatment on wettability and mechanical behaviour of flax/polypropylene composites. Compos Sci Technol 63(9):1247–1254

18. Li Z, Zhou X, Pei C (2011) Effect of sisal fiber surface treatment on properties of sisal fiber reinforced polylactide composites. Int J Polym Sci. doi:10.1155/2011/803428

19. Barré S, Benzeggagh M (1994) On the use of acoustic emission to investigate damage mechanisms in glass-fibre-reinforced polypropylene. Compos Sci Technol 52(3):369–376

20. Karmarkar A, Chauhan SS, Modak JM, Chanda M (2007) Mechanical properties of wood–fiber reinforced polypropylene composites. Effect of a novel compatibilizer with isocyanate functional group. Compos A Appl Sci Manuf 38(2):227–233

21. Ramsaroop A, Kanny K, Mohan T (2010) Fracture toughness studies of polypropylene-clay nanocomposites and glass fibre reinfoerced polypropylene composites. Mater Sci Appl 1(05):301

22. Saba N, Jawaid M, Alothman OY, Paridah MT (2016) A review on dynamic mechanical properties of natural fibre reinforced polymer composites. Constr Build Mater 106:149–159

23. Espert A, Vilaplana F, Karlsson S (2004) Comparison of water absorption in natural cellulosic fibres from wood and one-year crops in polypropylene composites and its influence on their mechanical properties. Compos Part A Appl Sci Manuf 35(11):1267–1276

24. Shakeri A, Raghimi M (2010) Studies on mechanical performance and water absorption of recycled newspaper/glass fiber-reinforced polypropylene hybrid composites. J Reinf Plast Compos 29(7):994–1005

25. Balakrishna NS, Ismail H, Othman N (2014) Polypropylene/rattan powder/kaolin hybrid composites: processing, mechanical and thermal properties. Polym Plast Technol Eng 53(5):451–458

26. Panthapulakkal S, Sain M (2007) Injection-molded short hemp fiber/glass fiber-reinforced polypropylene hybrid composites—mechanical, water absorption and thermal properties. J Appl Polym Sci 103(4):2432–2441

27. Lorenz H, Fritzsche J, Das A, Stöckelhuber KW, Jurk R, Heinrich G et al (2009) Advanced elastomer nano-composites based on CNT-hybrid filler systems. Compos Sci Technol 69(13):2135–2143

28. Yang K, Gu M (2010) Enhanced thermal conductivity of epoxy nanocomposites filled with hybrid filler system of triethylenetetramine-functionalized multi-walled carbon nanotube/silane-modified nano-sized silicon carbide. Compos A Appl Sci Manuf 41(2):215–221

29. Barus S, Zanetti M, Lazzari M, Costa L (2009) Preparation of polymeric hybrid nanocomposites based on PE and nanosilica. Polymer 50(12):2595–2600

30. Karsli NG, Aytac A (2011) Effects of maleated polypropylene on the morphology, thermal and mechanical properties of short carbon fiber reinforced polypropylene composites. Mater Des 32(7):4069–4073

31. Kim J, Kim D (2014) Compatibilizing effects of maleic anhydride-grafted-polypropylene (PP) on long carbon fiber-reinforced PP composites. J Thermoplast Compos Mater 28(11):1599–1611

32. Krump H, Luyt AS, Hudec I (2006) Effect of different modified clays on the thermal and physical properties of polypropylene-montmorillonite nanocomposites. Mater Lett 60(23):2877–2880

33. Kango S, Kalia S, Celli A, Njuguna J, Habibi Y, Kumar R (2013) Surface modification of inorganic nanoparticles for development of organic–inorganic nanocomposites—a review. Prog Polym Sci 38(8):1232–1261

34. Arao Y, Yumitori S, Suzuki H, Tanaka T, Tanaka K, Katayama T (2013) Mechanical properties of injection-molded carbon fiber/polypropylene composites hybridized with nanofillers. Compos A Appl Sci Manuf 55:19–26

35. Sattari M, Mirsalehi SA, Khavandi A, Alizadeh O, Naimi-Jamal MR (2015) Non-isothermal melting and crystallization behavior of UHMWPE/SCF/nano-SiO$_2$ hybrid composites. J Therm Anal Calorim 122(3):1319–1330

36. Tang J, Wang Y, Liu H, Belfiore LA (2004) Effects of organic nucleating agents and zinc oxide nanoparticles on isotactic polypropylene crystallization. Polymer 45(7):2081–2091

37. Layachi A, Frihi D, Satha H, Seguela R, Gherib S (2016) Non-isothermal crystallization kinetics of polyamide 66/glass fibers/carbon black composites. J Therm Anal Calorim 124(3):1319–1329

38. Samal SK, Mohanty S, Nayak SK (2008) Polypropylene–bamboo/glass fiber hybrid composites: fabrication and analysis of mechanical, morphological, thermal, and dynamic mechanical behavior. J Reinf Plast Compos 28(22):2729–2747
39. Li L, Li B, Hood MA, Li CY (2009) Carbon nanotube induced polymer crystallization: the formation of nanohybrid shish–kebabs. Polymer 50(4):953–965
40. Liang Y, Zheng G, Han W, Liu C, Chen J, Li Q et al (2011) Nano-hybrid shish–kebab: isotactic polypropylene epitaxial growth on electrospun polyamide 66 nanofibers via isothermal crystallization. Mater Lett 65(4):653–656
41. Jayanarayanan K, Bhagawan SS, Thomas S, Joseph K (2008) Morphology development and non isothermal crystallization behaviour of drawn blends and microfibrillar composites from PP and PET. Polym Bull 60(4):525–532
42. Jayanarayanan K, Thomas S, Joseph K (2012) Effect of blend ratio on the mechanical and sorption behaviour of polymer–polymer microfibrillar composites from low-density polyethylene and polyethylene terephthalate. J Reinf Plast Compos 31(8):549–562